Determination of the optical properties of anisotropic biological media using an isotropic diffusion model

Alwin Kienle
Corinna Wetzel
Institut für Lasertechnologien in der Medizin und Meßtechnik
Helmholtzstrasse 12
D-89081 Ulm, Germany
E-mail: alwin.kienle@ilm.uni-ulm.de

Andrea Bassi
Daniela Comelli
Paola Taroni
Antonio Pifferi
Politecnico di Milano
ULTRAS-CNR-INFM
IFN-CNR
Dipartimento di Fisica, P. L. da Vinci 32
I-20133 Milano, Italy

Abstract. We investigate anisotropic light propagation in biological tissue in steady-state and time domains. Monte Carlo simulations performed for tissue that consists of aligned cylindrical and spherical scatterers show that steady-state and time-resolved reflectance depends strongly on the measurement direction relative to the alignment of the cylinder axis. We examine the determination of optical properties using an isotropic diffusion model and find that in the time domain, in contrast to steady-state spatially resolved reflectance measurements, the obtained absorption coefficient does not depend on the measurement direction and is close to the true value. Contrarily, the derived reduced scattering coefficient depends strongly on the measurement direction in both domains. Measurements of the steady-state and time-resolved reflectance from bovine tendon confirm the theoretical findings. [DOI: 10.1117/1.2709864]

Keywords: anisotropic optical coefficients; diffusion equation; spatially resolved reflectance; time-resolved reflectance; tendon microstructure tendon collagen fibers.

Paper 06139R received Jun. 9, 2006; revised manuscript received Aug. 2, 2006; accepted for publication Aug. 24, 2006; published online Mar. 2, 2007.

1 Introduction

Knowledge of light propagation in biological tissue is important for a variety of optical applications in medicine. In applied theoretical models, it was normally assumed that the light propagation in biological tissue was isotropic.[1–4] In recent years, however, it has been increasingly recognized that light propagation in many tissue types is anisotropic due to their aligned microstructure. Thus, it is important to investigate errors when isotropic models are used to determine the optical properties of tissues that have an aligned microstructure.

Anisotropic light propagation in human tissue has been known for at least three decades. Walton, Outhwaite, and Pashley reported that disks of dentin taken from extracted human teeth show optical magnification and demagnification properties.[5] Light guiding in dentin and enamel was shown by Altshuler and Grisimow.[6] More recently, Marquez et al. found that optical properties determined from spatially resolved reflectance experiments on chicken breast depend on the measurement direction.[7] This was also reported by Nickell et al. for measurements on skin.[8] In addition, they found that when skin is illuminated with a pencil beam, the contour lines of spatially resolved reflectance are ellipses oriented perpendicular to the collagen fibers at small distances, whereas the orientation of the ellipses is parallel to the collagen fibers at large distances. They modeled the anisotropic light propagation with the Monte Carlo method, taking approximately the scattering by the collagen fibers into account. Recently, we explained the full pattern of spatially resolved reflectance from tissue that consists of an aligned cylindrical microstructure by implementing the exact phase functions of the cylinders into the Monte Carlo method and by comparing it to measurements on dentin and arteries.[9,10] The dependence of the anisotropic spatially resolved reflectance pattern on the polarization has been studied experimentally by Sviridov et al.[11] on skin and bone samples.

Calculations of anisotropic light propagation based on the diffusion theory[12] or random walk approach[13] were also performed. These models are valid in the diffusion regime, i.e., the ellipses of the spatially resolved reflectance at large distances can be explained. The random walk model was applied to analyze time-resolved reflectance measurements on anisotropic phantoms[14] and human skeletal muscle.[15]

We present investigations of steady-state and time-resolved reflectance from biological media that consist of cylindrical and spherical scatterers. We applied the Monte Carlo method using the phase functions of cylindrical scatterers to simulate the scattering by collagen fibers in tendon and by tubules in dentin, and, in addition, the Henyey-Greenstein phase function to characterize spherical scatterers. The optical properties were determined from spatially and time-resolved reflectance by fitting solutions of the isotropic diffusion equation to the Monte Carlo generated data and to measurements on bovine

Address all correspondence to Alwin Kienle, Institut für Lasertechnologien in der Medizin und Meßtechnik, an der Universität Ulm, Helmholtzstr.12, Ulm, D-89081 Germany; Tel: 0049 731 142924; Fax: 0049 731 142942; E-mail: alwin.kienle@ilm.uni-ulm.de

1083-3668/2007/12(1)/014026/9/$25.00 © 2007 SPIE

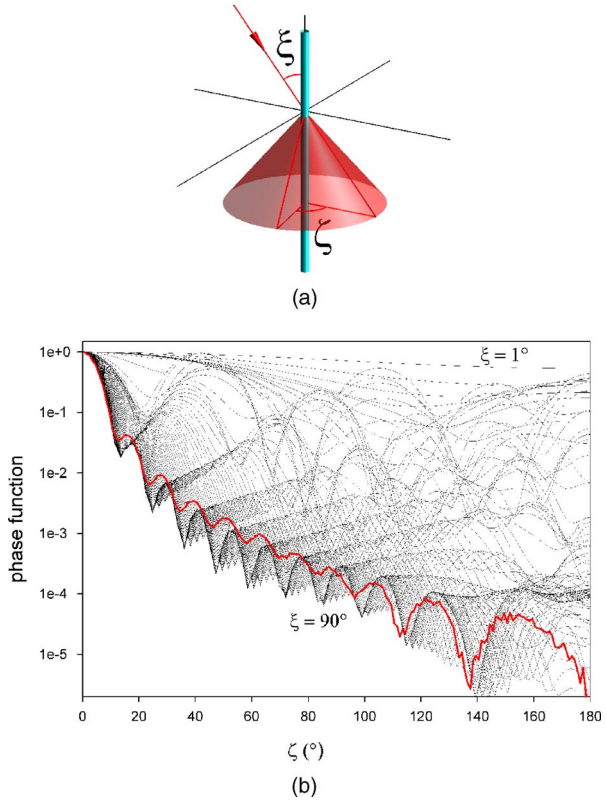

Fig. 1 (a) Scheme of light scattering characteristics by a cylinder. (b) Scattering phase functions of an infinitely long cylindrical collagen fiber in tendon for different incident angles ξ (1,2,3…90 deg) and $\lambda=800$ nm. The thick red curve shows the phase function of an isotropic distribution of the cylinders (color online only).

tendon representing a biological tissue with pronounced anisotropic optical properties. The optical coefficients obtained for reflectance in different directions relative to the cylindrical microstructure were explored and, if possible, compared to the true optical properties.

2 Theory

2.1 *Monte Carlo Method*

To calculate the light propagation in biological tissue that contains cylindrical scatterers, we modified our standard Monte Carlo code to implement the phase functions of cylindrical scatterers.[9,10] These phase functions were obtained from an analytical solution of the Maxwell equations for an infinitely long cylindrical scatterer at oblique incidence.[16] The calculations show that light incident at an angle ξ relative to the cylinder is scattered in a cone, with the cylinder as the axis of the cone having a half angle ξ [see Fig. 1(a)].[17] The scattering intensity around the cone for a certain ξ depends on the scattering direction defined by ζ. Figure 1(b) shows these scattering functions for all integer ξ values between 1 and 90 deg. For small ξ angles, the scattered intensity has a relative small dependence on ζ, whereas for large ξ values, the scattered intensity changes by several orders of magnitude. These calculations were performed for a collagen fiber in tendon having a diameter of $d=3$ μm,[18] a refractive index inside and outside the cylinder of 1.46 and 1.36, respectively.[18] Wavelengths of 633 and 800 nm [shown in Fig. 1(b)] were applied, because the measurements in the steady-state and time domains were performed at 633 and 800 nm, respectively. We note that the angle ζ is different from the normally used scattering angle θ. Only in the case of perpendicular incident light ($\xi=90$ deg) does ζ equal θ. In addition to the phase function, also the scattering efficiency Q_{sca} of the cylinder has to be considered.[17] Figure 2 shows the scattering efficiency for the collagen cylinder at 633 and 800 nm. It can be seen that Q_{sca} is much smaller in the direction parallel to the cylinder ($\xi=0$ deg) than perpendicular to the cylinder ($\xi=90$ deg).

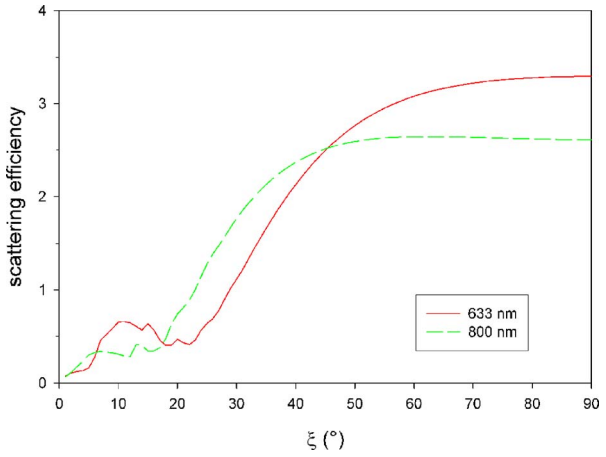

Fig. 2 Scattering efficiency versus ξ for the collagen fiber in tendon tissue at $\lambda=633$ and 800 nm.

The single scattering characteristics of the cylindrical scatterers were implemented into the Monte Carlo code to calculate the multiscattering found in biological tissue.[9,10] The cylindrical fibers were aligned parallel to the x axis in the semi-infinite turbid medium (see Fig. 3). The pencil light beam was incident in the z direction at $x=0$ mm, $y=0$ mm.

In addition to the cylindrical scatterers, we assumed that the tissue consists also of a certain concentration of spherical scatterers. (Or more generally, we regarded scatterers that have a rotationally symmetric phase function, for example, randomly aligned scatterers with an arbitrary shape for unpo-

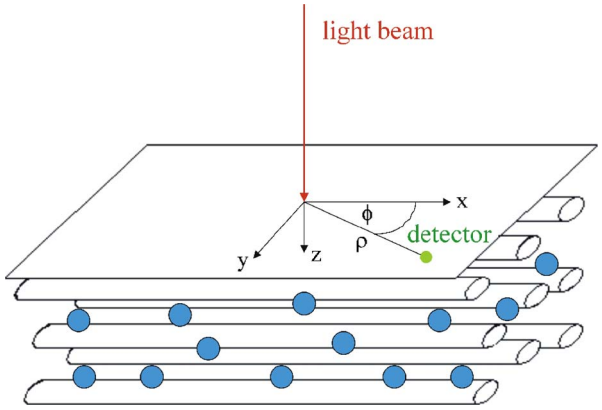

Fig. 3 Scheme of the turbid medium and some of the quantities used in the Monte Carlo simulation.

larized incident light.) For characterization of these particles, a Henyey-Greenstein function having an anisotropy factor of 0.8 was employed. The reduced scattering coefficient of the spherical particles is denoted by $\mu'_{s,\mathrm{iso}}$.

Using the Monte Carlo code, we calculated the spatially resolved reflectance $R(x,y)$ and the time-resolved reflectance $R(t,x,y)$ from the surface of the tissue. To demonstrate the anisotropic light propagation, we calculated also the reflectance in polar coordinates $R(\phi,\rho)$ and $R(t,\phi,\rho)$, where ρ is the distance between the source and the detector, and ϕ indicates the angle between the detector direction and the x axis (see Fig. 3). Reflectance data of adjacent ϕ values ($\Delta\phi = 20$ deg) and the corresponding sector mirrored at the x axis were averaged to reduced the statistical noise of the Monte Carlo simulations.

In Fig. 1(b), we depicted an additional curve (thick red line), which shows the phase function for an isotropic distribution of cylindrical tendon fibers. For the calculation of this phase function, it has to be taken into account that both the solid angle, for which a certain scattering function is valid, and the scattering efficiency depend on ξ. Alternatively, the phase function can be calculated from a Monte Carlo simulation with an isotropic distribution of the cylinders, considering only single scattering.

We used the phase function for an isotropic distribution of cylinders to check the Monte Carlo code. First, the anisotropy factor $g=\langle\cos(\theta)\rangle$ of the phase function was calculated. For example, for the phase function at $\lambda=800$ nm shown in Fig. 1(b), we obtained $g=0.989$. Then, the scattering coefficient for a certain ξ was computed with

$$\mu_s(\xi) = Q_{\mathrm{sca}}(\xi)dc_A, \tag{1}$$

where c_A is the density of the cylinders (number per area). The scattering coefficient averaged over all cylinder directions can be derived using

$$\langle\mu_s\rangle = \frac{\int_0^{\pi/2}\mu_s(\xi)\sin(\xi)d\xi}{\int_0^{\pi/2}\sin(\xi)d\xi} = \int_0^{\pi/2}\mu_s(\xi)\sin(\xi)d\xi. \tag{2}$$

Finally, the reduced scattering coefficient $\mu'_{s,\mathrm{cyl}}$ was obtained with

$$\mu'_{s,\mathrm{cyl}} = \langle\mu_s\rangle(1-g). \tag{3}$$

Here, the index cyl indicates the reduced scattering coefficient that is caused by an isotropic distribution of the considered cylinders.

In the time domain, we checked the Monte Carlo code by calculating $R(t,\rho)$ for an isotropic distribution of cylinders (with and without spherical scatterers). We fitted the time-resolved solution of the diffusion equation to the time-resolved reflectance simulated with the Monte Carlo method for different ϕ values. The obtained optical coefficients were compared with $\mu'_{s,\mathrm{cyl}}$ calculated with Eqs. (1)–(3) and the absorption coefficient used in the simulations. The optical properties agreed within 10%, which is a typical error due to the application of the diffusion approximation. Similar tests were performed in the steady-state domain, and again, the fitted optical properties agreed with those used in the Monte Carlo simulations within differences of 10%.

2.2 *Diffusion Theory*

For the determination of optical properties of biological media, it is normally assumed that the light propagation is isotropic. Usually a solution of the isotropic diffusion theory is applied to obtain the optical properties from spatially and time-resolved reflectance measurements.[2,19] To investigate the errors due to the application of these equations for tissue having an anisotropic light propagation, we fitted $R(\rho)$ and $R(t,\rho)$ for a semi-infinite homogeneous medium to the reflectance data obtained from the Monte Carlo simulations and to the experiments. The extrapolated boundary condition was used. For the calculation of $R(t,\rho)$, we applied a solution that considers the flux term only[20] [Eq. (5) in Ref. 21], whereas for $R(\rho)$, the slightly more complex solution considering the flux and the fluence term was applied [Eq. (8) in Ref. 21], because it matches the Monte Carlo simulations better than the solution that considers only the flux term. In the time domain, however, the solutions for both boundary conditions agree similarly to time-resolved Monte Carlo simulations.[21]

In the steady-state domain, $R(\rho)$ was fitted to Monte Carlo data for distances between $\rho=1$ mm and $\rho=16$ mm for each ϕ direction. Smaller values than $\rho=1$ mm were excluded from the calculations because of the breakdown of the diffusion solution.[21] The end point of the fitting range was chosen by considering the dynamical range of our charge-coupled device (CCD) camera. In the time domain, the start time of the fitting range was at the peak of the $R(t,\rho)$ curves obtained from the Monte Carlo simulations. The end time was chosen at the time when $R(t,\rho)$ was approximately two and a half orders of magnitudes smaller than at the peak of $R(t,\rho)$ for the time-resolved reflectance averaged over all ϕ directions. In general, we found for both domains that different fitting ranges did only marginally change the derived optical properties. The weights used in the fitting routine were calculated using Poisson statistics.

3 Materials and Methods

The spatially and time-resolved reflectance measurements were performed on bovine achilles tendon, which was obtained from the butcher a few days before measurements and stored in the freezer (−20 °C) in the intermediate time. For the measurements it was thawed out to room temperature. The sample size was unmodified and was approximately $50\times30\times15$ mm in x, y, and z directions; with the collagen fibers, clearly visible to the eye, running parallel to the longest side (compare Fig. 3).

The measurements of the spatially resolved reflectance were performed similarly as described in detail elsewhere.[22] Briefly, a HeNe laser at $\lambda=633$ nm was approximately perpendicular incident to the biological tissue. The laser beam was focused at the tissue boundary having a diameter of 50 μm. The remitted light was imaged onto a 16-bit CCD camera cooled down to −65 °C. No polarizers were used in the measurement setup. For each experiment, a background

measurement was performed with the laser switched off and subtracted from the measurement with the laser beam switched on.

Time-resolved reflectance measurements were performed with a home-built spectroscopy system.[23] An actively mode-locked titanium: sapphire laser provided light at $\lambda = 800$ nm. A couple of plastic-glass fibers (core diameter 1 mm) delivered light into the sample and collected the reflected photons at a distance ρ. A double microchannel plate photomultiplier tube (R1564U, Hamamatsu, Japan) with an S1 surface and a PC board for time-correlated single-photon counting were used for detection. A small fraction of the incident beam was split off, coupled to a fiber, and fed directly to the photomultiplier tube for on-line recording of the instrumental response function (IRF). Overall, the IRF was <60 ps full width half maximum (FWHM). The reduced scattering and absorption coefficients were obtained from the same solution of the isotropic diffusion equation for a semi-infinite homogeneous medium, as used in the best fit of Monte Carlo simulations. The theoretical curve was convoluted with the IRF and normalized to the area of the experimental curve.

A simultaneous estimate of μ_s' and μ_a was achieved by best fitting with a nonlinear least square method the measured time-resolved reflectance curves to the reflectance $R(t,\rho)$. For determination of μ_s' and μ_a, two different fitting ranges were used, although in both cases both parameters were fitted. The fitting range for the assessment of μ_s' was taken from the peak channel down to 1% of the peak value. For the retrieval of μ_a, we followed a different strategy to face the problems related to the variation of the fitted μ_s' along the different directions. In fact, also in isotropic media, a scattering-to-absorption coupling is observed for low interfiber distances and low μ_s' values ($\rho \leq 10$ mm, $\mu_s < 0.5$ mm^{-1}). This effect is possibly due to the inaccuracy of the theoretical model convoluted with the instrumental response function.[24] In particular, for the system used in the present study, when decreasing the scattering coefficient from 1.2 mm^{-1} down to 0.4 mm^{-1} for $\mu_a = 0.006$ mm^{-1} and $\rho = 10$ mm, the fitted μ_a is altered by up to 30% (data not shown). This is possibly related to the fact that upon decreasing μ_s', the fitting range shrinks toward earlier photons. Contrarily, if the fitting range is kept fixed for all measurements to the interval obtained for the highest μ_s', then the scattering-to-absorption coupling is reduced. In particular, for our system, fixing the range from 100% down to 1% of the peak value of the highest μ_s' measurement, the coupling is $<20\%$. Moving toward longer lived photons, i.e., from 50% down to 1%, the coupling gets $<10\%$. Consequently, the fitted μ_a for the anisotropic measurements were analyzed applying this latter range.

Measurements on bovine tendon were performed at different angles $\phi = 0, 20, \ldots, 340$ deg with a fixed interfiber distance $\rho = 10$ mm. 16 measurements were repeated in each position, with acquisition time of 1 s for each position and count rate of 2×10^5 counts/s. The optical properties obtained from the fitting for all measurements performed in the same experimental condition were averaged.

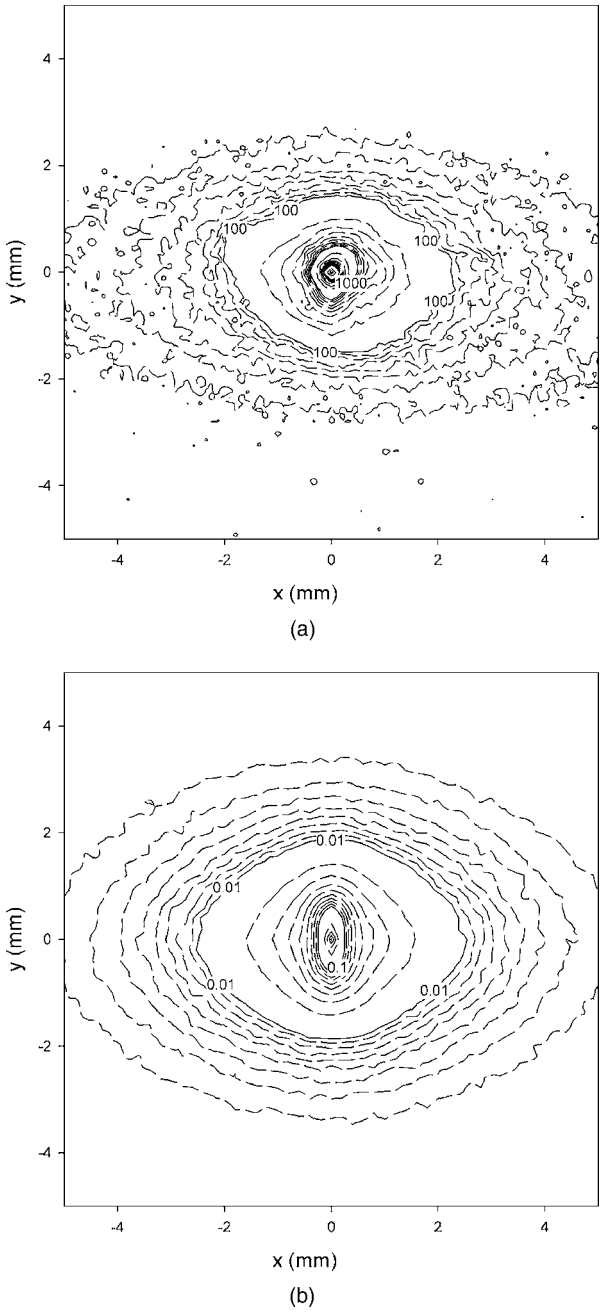

Fig. 4 Spatially resolved reflectance from tendon tissue obtained (a) from measurements using a CCD camera and (b) from Monte Carlo simulations. Isoreflectance contour lines are shown (a) in number of counts and (b) in mm^{-2}.

4 Results

4.1 *Steady-State Spatially Resolved Reflectance*

Figure 4(a) shows the spatially resolved reflectance $R(x,y)$ obtained from the measurements on the tendon sample. The tendon's collagen fibers were approximately aligned in the x direction. The contour lines of $R(x,y)$ have an elliptical shape oriented perpendicular to the collagen direction at small distances from the incident source, whereas at large distances the ellipses are oriented parallel to the direction of the collagen fibers.

In Fig. 4(b), $R(x,y)$ obtained from the Monte Carlo simulations are depicted. In the calculation, the density of the collagen fibers was set to $c_A=12700\ \mathrm{mm}^{-2}$, which would result in a reduced scattering coefficient of $\mu'_{s,\mathrm{cyl}}=1\ \mathrm{mm}^{-1}$, if the cylinders were distributed isotropically. For the spherical scatterers and for the absorption coefficient, we assumed $\mu'_{s,\mathrm{iso}}=0.8\ \mathrm{mm}^{-1}$ and $\mu_a=0.01\ \mathrm{mm}^{-1}$, respectively. The results from the Monte Carlo simulation show good qualitative agreement with the measurements. The orientations of the ellipses at small and large distances are the same as in the experiment. By changing the ratio between $\mu'_{s,\mathrm{cyl}}/\mu'_{s,\mathrm{iso}}$, the axis ratio of the ellipses can be altered (see Sec. 5).

Figure 5 shows the absorption and reduced scattering coefficients obtained by fitting the solution of the diffusion equation for $R(\rho)$ to the Monte Carlo results shown in Fig. 4(b) for different ϕ directions. The derived optical coefficients were mirrored at the x axis, because the simulated data were summed up as described in Sec. 2. A strong dependence of the derived absorption and reduced scattering coefficients on the measurement direction ϕ can be seen. This anisotropy of the optical properties was already reported.[7,8,10] However, with the results presented here, the fitted optical coefficients can be compared with the true optical properties of the turbid medium. For example, the absorption coefficient used in the Monte Carlo simulation is $\mu_a=0.01\ \mathrm{mm}^{-1}$ throughout the semi-infinite turbid medium, whereas the derived μ_a changes from $\mu_a=0.0044\ \mathrm{mm}^{-1}$ at $\phi=90$ deg to $\mu_a=0.0167\ \mathrm{mm}^{-1}$ at $\phi=170$ deg. The reduced scattering coefficient varies between $\approx 0.8\ \mathrm{mm}^{-1}$, which is close to $\mu'_{s,\mathrm{iso}}$ and $3.6\ \mathrm{mm}^{-1}$. Obviously, using the diffusion equation, the derived absorption coefficients have large differences compared to the true value. When the spatially resolved reflectance is averaged over all ϕ angles, the fitted optical coefficients are $\mu_a=0.0051\ \mathrm{mm}^{-1}$ and $\mu'_s=1.71\ \mathrm{mm}^{-1}$. Thus, even in this case the derived μ_a has a large error.

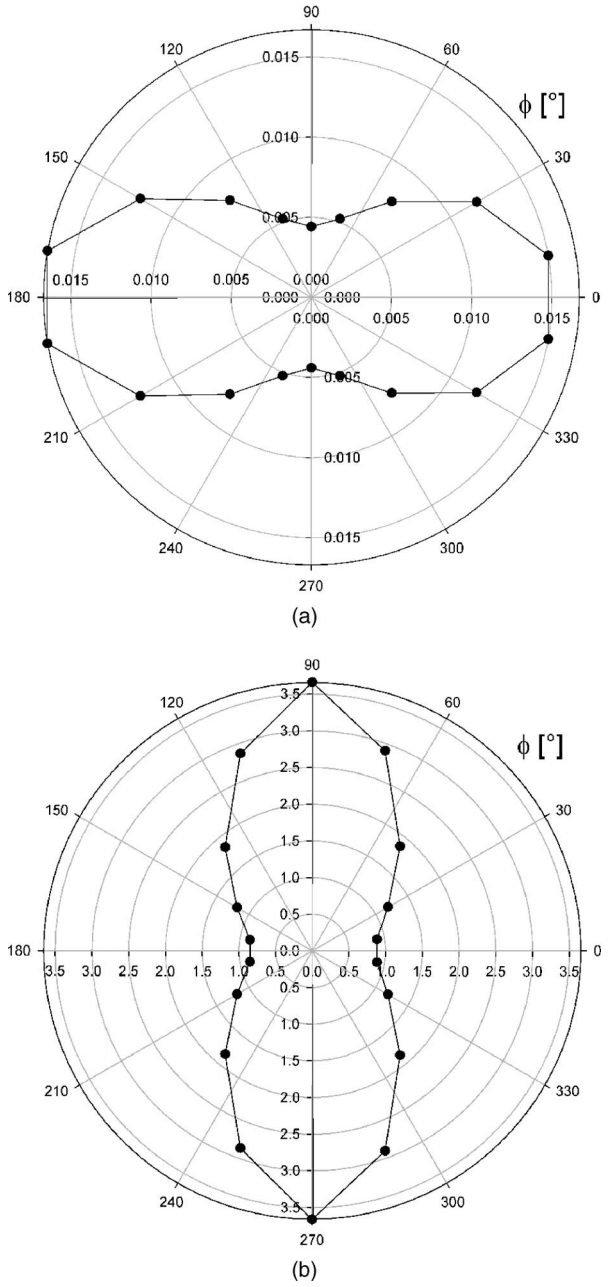

Fig. 5 Absorption coefficient (mm^{-1}) and (b) reduced scattering coefficient (mm^{-1}) obtained by fitting the solution of the diffusion equation to the Monte Carlo generated steady-state spatially resolved reflectance from a turbid medium consisting of collagen fibers in tendon and spherical scatterers for different ϕ directions. The optical properties are mirrored at the x axis, because these data were summed up in the Monte Carlo simulations.

4.2 *Time-Domain Reflectance*

Figure 6 shows the time-resolved reflectance obtained from Monte Carlo simulations at a distance of $\rho=9.5$ mm from the source using the phase functions for a collagen fiber in tendon tissue at $\lambda=800$ nm. As in the steady-state domain, we used $\mu'_{s,\mathrm{cyl}}=1\ \mathrm{mm}^{-1}$, $\mu'_{s,\mathrm{iso}}=0.8\ \mathrm{mm}^{-1}$, and $\mu_a=0.01\ \mathrm{mm}^{-1}$. Large differences between the $R(t,\rho)$ curves in different directions can be seen. The smaller ϕ, the more photons are remitted at early times. However, at long times the curves converge to one curve. The experimental reflectance measured from the tendon shows qualitatively the same characteristics, when deconvolved with the instrumental response function (figure not shown). As the characteristics of $R(t,\rho)$ at long t are mainly determined by the absorption coefficient, it can be hypothesized that with time-resolved reflectance measurements, the absorption coefficient can be correctly obtained using an isotropic model.

To check this statement, we fitted the solution of the diffusion theory for the time-resolved reflectance to the $R(t,\rho)$ obtained from the Monte Carlo simulation at different ϕ directions at a distance of $\rho=9.5$ mm. Figure 7(a) shows that the fitted absorption coefficients do not depend on the measurement direction except for the statistics of the Monte Carlo simulations. The absolute values are in average 10% larger than the true absorption coefficient. This is in part due to the relative large noise of the simulations (compare Fig. 6). We found that increasing the simulation time results in a small decrease of the determined absorption coefficient and, thus, in a smaller difference to the true absorption coefficient. In addition, we observed that the larger the distance between source and detector, the closer the obtained absorption coefficient is to the correct value. Contrarily, for small distances

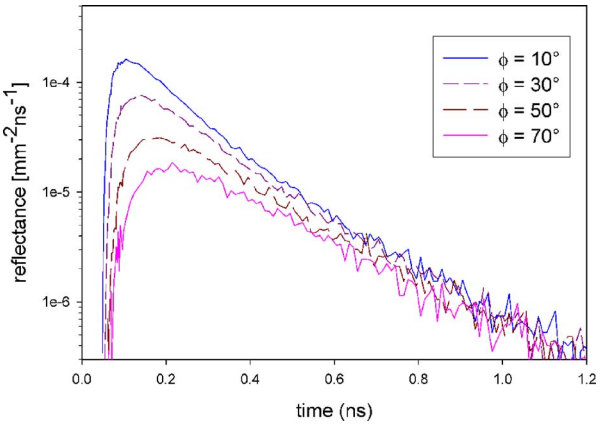

Fig. 6 Monte Carlo simulations of the time-resolved reflectance from a turbid medium consisting of aligned collagen fibers in tendon and of spherical scatterers for four different directions of the detector (ϕ =10, 30, 50, and 70 deg).

between source and detector ($\rho \gg 1/\mu_s'$), we found that the fitted absorption coefficient depends on the measurement direction, but for these distances the diffusion approximation breaks down anyway (at least for small times).

The derived reduced scattering coefficient, in contrast, depends strongly on the measurement direction. In a direction parallel to the cylinders, it is more than three times smaller than perpendicular to the cylinders. Thus, all the anisotropy of the light propagation is embodied in the reduced scattering coefficient. In general, the larger the ratio between $\mu_{s,\mathrm{cyl}}'$ and $\mu_{s,\mathrm{iso}}'$, the larger are the differences of the fitted reduced scattering coefficient for different directions, i.e., the larger the anisotropy of the light propagation.

Figure 8 reports the absorption and reduced scattering coefficients derived from the best fit of time-resolved reflectance measurements performed on bovine tendon. The estimated μ_s' shows a strong dependence on the measurement direction. Specifically, the ratio between values derived from measurements performed normal and parallel to the fiber direction is 10.6, while for μ_a it is just 1.16 when the fixed fitting range is adopted, as described in Sec. 3. If the free fitting range (same as for μ_s') is used, the ratio for μ_a is increased to 1.38, yet is till lower than the scattering variation.

We also performed Monte Carlo simulations for cylinders other than collagen fibers. Figure 9 shows the obtained optical properties derived by fitting the time-resolved solution of the diffusion equation to simulation results calculated for dental tubules. For these cylindrical channels, we used a diameter of d=2 μm, and a refractive index inside and outside the cylinders of n_i=1.33 and n_o=1.52, respectively. The optical coefficients used in the Monte Carlo simulations are $\mu_{s,\mathrm{cyl}}'$ =0.66 mm^{-1}, $\mu_{s,\mathrm{iso}}'$=1 mm^{-1}, and μ_a=0.03 mm^{-1}. For this simulation, the cylindrical tubules are only approximately aligned in the x direction having a standard deviation of 10 deg around the x axis. The distance between source and detector is ρ=9.5 mm.

As for the turbid medium containing collagen fibers, the determined absorption coefficient is isotropic within the statistical nature of the Monte Carlo simulations. The differences of the fitted μ_a are in average smaller than 10 % compared to

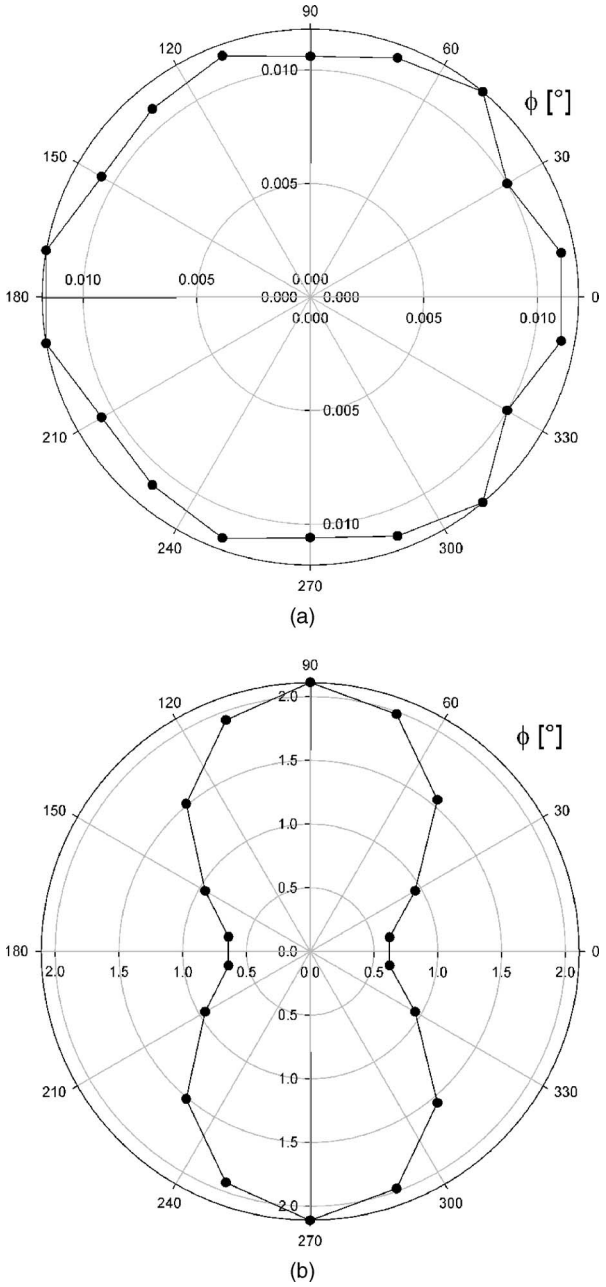

Fig. 7 (a) Absorption coefficient (mm^{-1}) and (b) reduced scattering coefficient (mm^{-1}) obtained by fitting the solution of the diffusion equation to the Monte Carlo generated time-resolved reflectance from a turbid medium consisting of aligned collagen fibers in tendon and spherical scatterers for different ϕ directions. The optical properties are mirrored at the x axis.

the value used in the Monte Carlo simulations, whereas the values of the fitted reduced scattering coefficients depend on the measuring direction. Here, the anisotropy of the fitted μ_s' is smaller than for the data shown in Fig. 7. This is mainly due to the smaller ratio of $\mu_{s,\mathrm{cyl}}'$ and $\mu_{s,\mathrm{iso}}'$. Also, in general, the not exact alignment in the x direction causes a more isotropic light propagation.

5 Discussion

We investigated anisotropic light propagation in biological media in steady-state and time domains. We showed experi-

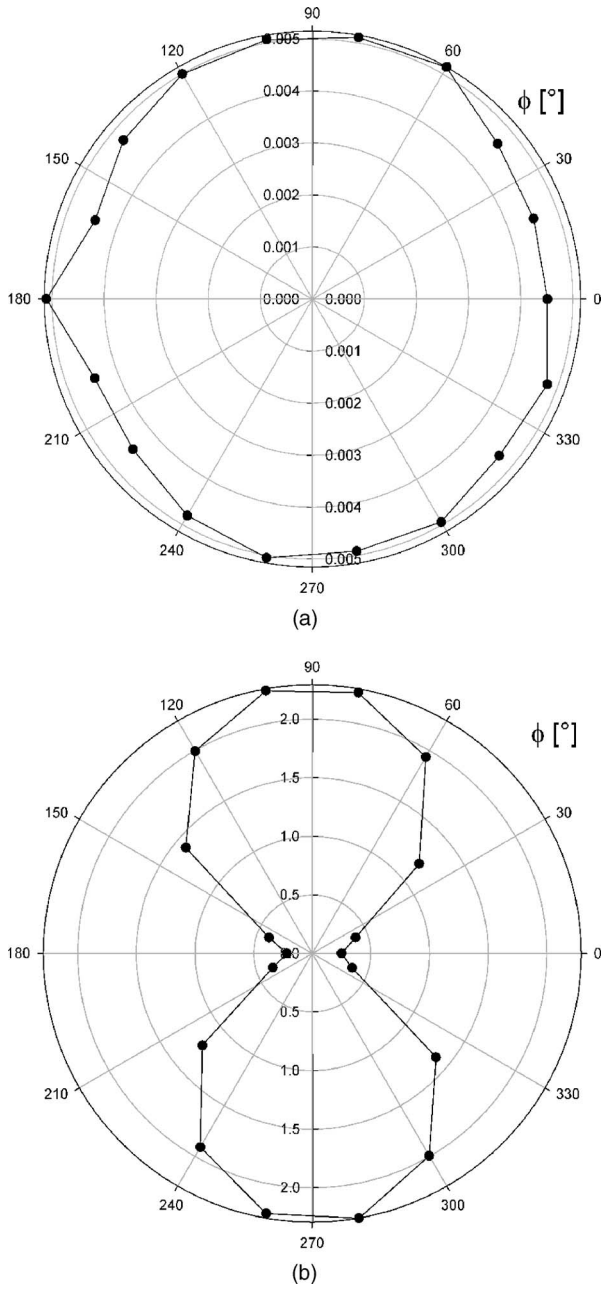

Fig. 8 (a) Absorption coefficient (mm^{-1}) and (b) reduced scattering coefficient (mm^{-1}) obtained by fitting the solution of the diffusion equation to the time-resolved measurements on tendon for different ϕ directions.

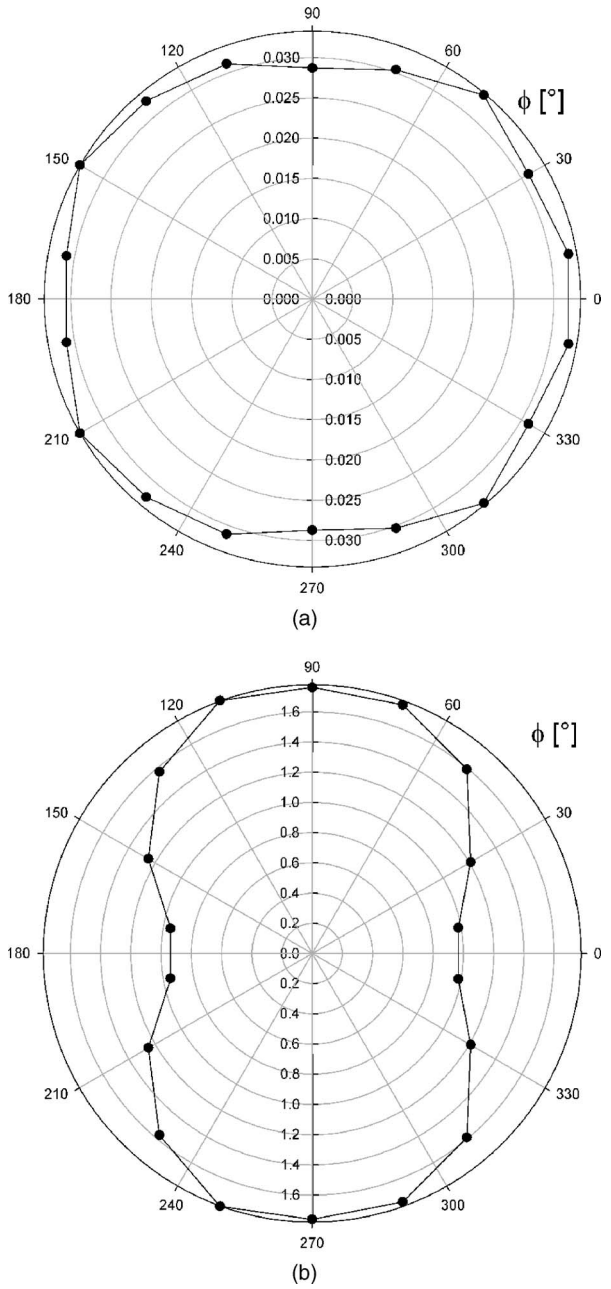

Fig. 9 (a) Absorption coefficient (mm^{-1}) and (b) reduced scattering coefficient (mm^{-1}) obtained by fitting the solution of the diffusion equation to the Monte Carlo generated time-resolved reflectance from a turbid medium consisting of cylindrical and spherical scatterers for different ϕ directions. The optical and geometrical parameters for the cylinders were those of dental tubules.

mentally and theoretically that in both domains the reflectance depends strongly on the measurement direction relative to the aligned microstructure.

In the theoretical study it was assumed that the turbid medium consists of both aligned cylindrical and spherical scatterers. Scattering at the cylindrical microstructure causes the anisotropy in the light propagation. More quantitatively, by performing a series of Monte Carlo simulations, we found that the degree of anisotropy depends mainly on the ratio between $\mu'_{s,\mathrm{cyl}}$ and $\mu'_{s,\mathrm{iso}}$. Further investigations showed that anisotropic light propagation is practically not influenced by the absorption coefficient (data not shown). Additionally, two different aligned microstructures were examined, describing collagen fibers in tendon and tubules in dentin. We found that the influence of the optical and geometrical properties of the cylinders on the anisotropic light propagation is marginal as long as $\mu'_{s,\mathrm{cyl}}$ is the same.

We examined errors in determining the optical coefficients of turbid media having an anisotropic microstructure when commonly applied isotropic solutions of the diffusion equation are employed. In the steady-state domain, it was found

that the reduced scattering and absorption coefficients derived with the diffusion solutions depend strongly on the measurement direction on the surface, as was already reported in the literature.[7,8,10] In this study, however, we presented a quantitative comparison with the true optical properties. Even when the ϕ dependence is averaged over the entire 360 deg, the derived optical properties have large errors. Thus, in the steady-state domain the determination of the optical properties using an isotropic model can cause large errors when applied to tissue having anisotropic optical properties, at least if a part of the spatially resolved reflectance is measured at distances for which $\rho \not\gg 1/\mu_s'$.

In contrast, in the time domain it was shown theoretically and with experiments on tendon tissue that the fitted absorption coefficient does not depend on the measuring direction, if the distance between the source and detector is sufficiently large ($\rho \gg 1/\mu_s'$). For smaller distances, coupling of the derived absorption and the reduced scattering coefficients can be seen as similar to the steady-state domain.

In *in vivo* investigations, the anisotropy of the fitted optical coefficients is probably smaller, because normally many different tissue types with a different aligned microstructure are involved.

The elliptical shapes of the experimental and theoretical isointensity lines of the spatially resolved reflectance from the tendon agreed qualitatively. A closer inspection of Fig. 4, however, reveals that the experimental ellipses have a larger ratio of the large and small semi-axes of the ellipses at large distances, whereas this ratio is smaller at small distances ρ compared to theoretical ellipses. By decreasing the isotropic part of the reduced scattering coefficient $\mu_{s,\mathrm{iso}}'$, in the Monte Carlo simulations, the ellipses at large distances are elongated, and thus, match the experimental contour lines. However, also ellipses at small distances will be elongated in the simulations, and this does not correspond to the experimental results. This discrepancy is probably due to the wiggling form of the collagen fibers in tendon. Thus, although they are globally aligned in one direction locally, a collagen fiber exhibits different directions. Presumably, this structure will result in smaller ellipses at small distances. Thus, the experimental results could be better reproduced by considering this wiggling structure of the collagen fibers and by decreasing $\mu_{s,\mathrm{iso}}'$ in the Monte Carlo simulations. This also implicates that the collagen fibers are by far the most important scatterers in tendon.

The angular dependence of the optical coefficients of bovine tendon as derived from the fit of time-resolved reflectance measurements is similar to what was obtained from Monte Carlo simulations. Actually, the anisotropy of the fitted μ_s' is even more marked for tendon measurements. However, its real optical properties were not known, nor did we consider the wiggling form of the tendon fibers. Consequently, no attempt of quantitative comparisons was made. The fitted μ_a of bovine tendon shows some systematic change in the measurement direction, even though it is much smaller than observed for μ_s'. Specifically, higher μ_a values are obtained when the measurement direction is normal to the collagen fibers (ϕ=90). This may be at least in part due to the finite size of the sample that is not accounted for by the diffusion model used to estimate the optical coefficients. Indeed, photons escaping from the boundary may lead to higher values of the fitted μ_a. Moreover, care must be taken when the difference between the scattering coefficients along the two orthogonal directions is high, and in particular, for very small values of the lower scattering coefficient. In this case it is possible to adopt the same strategies devised for isotropic media to handle low scattering values, such as excluding the early photons from the fit, or using a larger interfiber distance for the lower μ_s'.

In this work we used the solution of the isotropic diffusion equation to recover the optical properties. Recently, the solution of an anisotropic diffusion equation has been presented.[12] By applying this anisotropic model, the turbid medium containing cylinders in the x direction can be characterized with two different reduced scattering coefficients, one for the x direction and the other for the y and z directions. In the limit of measurements far from the incident source ($\rho \gg 1/\mu_s'$), the solutions of the anisotropic diffusion equation for the reflectance on the x and y axes are practically the same as the solution of the time-dependent isotropic diffusion equation. Thus, the optical coefficients derived for measurements in the time domain on the x and y axes using the isotropic model deliver also the reduced scattering coefficients needed for the anisotropic model.

For spatially resolved steady-state reflectance, however, it is in many cases difficult to fulfill the condition that the measurements have to be performed far from the source. As a result, we do have a coupling between the absorption and reduced scattering coefficients (compare Fig. 5). Yet determining the optical properties using several spatially resolved steady-state measurements performed in different directions in one fit, and by applying the anisotropic diffusion equation, might improve the accuracy of the obtained optical properties.

Acknowledgment

Financial support by the access to research infrastructure activity in the Sixth Framework Programme of the EU (contract RII3-CT-2003-506350, Laserlab Europe) for conducting the research is gratefully acknowledged.

References

1. A. Ishimaru, *Wave Propagation and Scattering in Random Media*, Academic Press, New York (1978).
2. M. S. Patterson, B. Chance, and B. C. Wilson, "Time resolved reflectance and transmittance for the noninvasive measurement of tissue optical properties," *Appl. Opt.* **28**, 2331–2336 (1989).
3. S. R. Arridge, M. Cope, and D. T. Delpy, "The theoretical basis for the determination of optical pathlength in tissue: Temporal and frequency analysis," *Phys. Med. Biol.* **37**, 1531–1560 (1992).
4. A. Torricelli, A. Pifferi, L. Spinelli, R. Cubeddu, F. Martelli, S. Del Bianco, and G. Zaccanti, "Time-resolved reflectance at null source-detector separation: Improving contrast and resolution in diffuse optical imaging," *Phys. Rev. Lett.* **95**, 078101 (2005).
5. R. E. Walton, W. C. Outhwaite, and D. F. Pashley, "Magnification - An interesting optical property of dentin," *J. Dent. Res.* **55**, 639–642 (1976).
6. G. B. Altshuler and V. M. Grisimov, "New optical effects in the human hard tooth tissues," *Proc. SPIE* **1353**, 97–102 (1989).
7. G. Marquez, L. V. Wang, S. P. Lin, J. A. Schwartz, and S. L. Thomsen, "Anisotropy in the absorption and scattering spectra of chicken breast tissue," *Appl. Opt.* **37**, 798–804 (1998).
8. S. Nickell, M. Hermann, M. Essenpreis, T. J. Farrell, U. Krämer, and M. S. Patterson, "Anisotropy of light propagation in human skin," *Phys. Med. Biol.* **45**, 2873–2886 (2000).

9. A. Kienle, F. K. Forster, R. Diebolder, and H. Hibst, "Light propagation in dentin: Influence of microstructure on anisotropy," *Phys. Med. Biol.* **48**, N7–N14 (2003).
10. A. Kienle, F. K. Forster, and R. Hibst, "Anisotropy of light propagation in biological tissue," *Opt. Lett.* **29**, 2617–2619 (2004).
11. A. Sviridov, V. Chernomordik, M. Hassan, A. Russo, A. Eidsath, P. Smith, and A. H. Gandjbakhche, "Intensity profiles of linearly polarized light backscattered from skin and tissue-like phantoms," *J. Biomed. Opt.* **10**, 014012 (2005).
12. J. Heino, S. Arridge, J. Sikora, and E. Somersalo, "Anisotropic effects in highly scattering media," *Phys. Rev. E* **68**, 031908 (2003).
13. L. Dagdug, G. H. Weiss, and A. H. Gandjbakhche, "Effects of anisotropic optical properties on photon migration in structured tissue," *Phys. Med. Biol.* **48**, 1361–1370 (2003).
14. J. C. Hebden, J. J. G. Guerrero, V. Chernomordik, and A. H. Gandjbakhche, "Experimental evaluation of an anisotropic scattering model of a slab geometry," *Opt. Lett.* **29**, 2518–2520 (2004).
15. T. Binzoni, C. Courvoisier, R. Giust, G. Tribillon, T. Gharbi, J. C. Hebden, T. S. Leung, J. Roux, and D. T. Delpy, "Anisotropic photon migration in human skeletal muscle," *Phys. Med. Biol.* **51**, N79–N90 (2006).
16. H. A. Yousif and E. Boutros, "A FORTRAN code for the scattering of EM plane waves by an infinitely long cylinder at oblique incidence," *Comput. Phys. Commun.* **69**, 406–414 (1992).
17. C. F. Bohren and D. R. Huffman, *Absorption and Scattering of Light by Small Particles*, John Wiley and Sons, New York (1983).
18. R. Drezek, A. Dunn, and R. Richards-Kortum, "Light scattering from cells: Finite-difference time-domain simulations and goniometric measurements," *Appl. Opt.* **38**, 3651–3661 (1999).
19. T. J. Farrell, M. S. Patterson, and B. C. Wilson, "A diffusion theory model of spatially resolved, steady-state diffuse reflectance for the noninvasive determination of tissue optical properties *in vivo*," *Med. Phys.* **19**, 879–888 (1992).
20. R. C. Haskell, L. O. Svaasand, T. T. Tsay, T. C. Feng, M. S. McAdams, and B. J. Tromberg, "Boundary conditions for the diffusion equation in radiative transfer," *J. Opt. Soc. Am. A* **11**, 2727–2741 (1994).
21. A. Kienle and M. S. Patterson, "Improved solutions of the steady-state and the time-resolved diffusion equations for reflectance from a semi-infinite turbid medium," *J. Opt. Soc. Am. A* **14**, 246–254 (1997).
22. A. Kienle, L. Lilge, M. S. Patterson, R. Hibst, R. Steiner, and B. C. Wilson, "Spatially resolved absolute diffuse reflectance measurements for noninvasive determination of the optical scattering and absorption coefficients of biological tissue," *Appl. Opt.* **35**, 2304–2314 (1996).
23. R. Cubeddu, A. Pifferi, P. Taroni, A. Torricelli, and G. Valentini, "Non-invasive absorption and scattering spectroscopy of bulk diffusive media: An application to the optical characterization of human breast," *Appl. Phys. Lett.* **74**, 874–876 (1999).
24. R. Cubeddu, A. Pifferi, P. Taroni, A. Torricelli, and G. Valentini, "Experimental test of theoretical models for time-resolved reflectance," *Med. Phys.* **23**, 1625–1634 (1996).